High Resolution Microwave Frequency Measurement Using a Dual-Parallel Mach-Zehnder Modulator

Article *in* IEEE Microwave and Wireless Components Letters · November 2013

DOI: 10.1109/LMWC.2013.2280638

Shilong Pan
Nanjing University of Aeronautics & Astronautics

High Resolution Microwave Frequency Measurement Using a Dual-Parallel Mach–Zehnder Modulator

Hualin Zhang and Shilong Pan, *Member, IEEE*

***Abstract*—A novel microwave frequency measurement scheme based on a dual-parallel Mach-Zehnder modulator (DPMZM) is proposed and demonstrated. By simply adjusting the bias voltage of the DPMZM, the measurement range can be divided into several parts and each part has very high resolution. Thus, the system can be used in a two-stage instantaneous frequency measurement scheme, in which the first stage coarsely determines the frequency band of the intercepted microwave signal, and then the proposed scheme measures the frequency with high resolution. An experiment is performed. Instantaneous frequency measurement with a frequency measurement range of 2.3–18.7 GHz and a measurement resolution of ± 0.20 GHz is achieved.**

***Index Terms*—Dual-parallel Mach-Zehnder modulator (DPMZM), instantaneous frequency measurements (IFM), microwave photonics.**

I. Introduction

In a defense system, an instantaneous frequency measurement (IFM) receiver is needed to measure the carrier frequency of an intercepted microwave signal before passing it to a specialized receiver for further signal processing [1]. Thanks to the distinctive advantages in terms of instantaneous measurement, large measurement range, small size, low power consumption, and immunity to electromagnetic interference, photonic-assisted microwave frequency measurement has attracted great interests recently. A lot of methods were proposed [2]–[10], but most of them have problem of either large measurement range with low resolution or high resolution with small measurement range [2]–[5]. To overcome this problem, one efficient approach is to divide a large measurement range into several parts and measure each part in serial or in parallel. Previously, Zou *et al.* implemented a photonic-assisted microwave frequency measurement scheme with tunable measurement range using a Mach-Zehnder modulator (MZM) and two/three lasers with wavelength tuning ranges as large as 130 nm [6], which is too expensive to be used in practical systems. Li *et al.* demonstrated a reconfigurable IFM system based on a conventional MZM and a dual-parallel MZM (DPMZM) [7], but two modulators have to be used. In [8], [9], the frequency measurement range of the microwave frequency measurement systems can be adjusted by tuning the wavelength of the laser or the dispersion of the dispersive elements. However, calibration is needed to ensure the measurement accuracy, especially when the measurement range is changed, making the system unable to perform instantaneous measurement.

In this letter, a novel microwave frequency measurement scheme based on a DPMZM is proposed and demonstrated, which can achieve very high resolution in a specific measurement range by simply adjusting the bias voltage of the DPMZM. Optimized resolution for a specific measurement range is achieved.

Manuscript received May 27, 2013; revised August 07, 2013; accepted August 27, 2013. Date of publication September 25, 2013; date of current version November 04, 2013. This work was supported in part by the National Basic Research Program of China (2012CB315705), the Jiangsu Provincial Funds for Distinguished Young Scientists (BK2012031), the Fundamental Research Funds for the Central Universities (NE2012002, NP2013101), a Project Funded by the Priority Academic Program Development of Jiangsu Higher Education Institutions, and the funds of department of education of Fujian Province (JB12143).

H. Zhang is with the Microwave Photonics Research Laboratory, College of Electronic and Information Engineering, Nanjing University of Aeronautics and Astronautics, Nanjing, 210016, China and also with the Department of Physics and Electronic Information Engineering, Minnan Normal University, Zhangzhou, 363000, China.

S. Pan is with the Microwave Photonics Research Laboratory, College of Electronic and Information Engineering, Nanjing University of Aeronautics and Astronautics, Nanjing 210016, China. (e-mail: pans@ieee.org).

Color versions of one or more of the figures in this letter are available online at http://ieeexplore.ieee.org.

Digital Object Identifier 10.1109/LMWC.2013.2280638

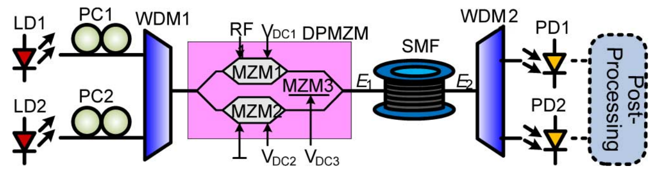

Fig. 1. Schematic of the proposed microwave frequency measurement system based on a DPMZM.

II. Principle

The schematic of the proposed system for microwave frequency measurement is shown in Fig. 1, which includes two laser diodes (LDs), two polarization controllers (PCs), two wavelength-division multiplexers (WDMs), a dual-parallel Mach-Zehnder modulator (DPMZM), a section of single-mode fiber (SMF), and two photodetectors (PDs). Two lightwaves with different wavelengths are combined by WDM1 and then sent to the DPMZM. The microwave signal with its frequency to be identified is applied to the DPMZM via one of its RF ports. The upper arm of the DPMZM (i.e., MZM1) is biased at the minimum transmission point to implement carrier suppressed double sideband (CS-DSB) modulation. The other RF port of the DPMZM is grounded, and the bottom arm of the DPMZM (i.e., MZM2) is biased at the maximum transmission point. The output signal from the DPMZM is sent to the SMF which is used to introduce dispersion-induced microwave power penalties to the two wavelengths. The two wavelengths are then separated by WDM2 and converted back to the electrical domain by the two PDs. The microwave powers are measured, compared and used to estimate the microwave frequency in a post-processing stage.

Mathematically, when a lightwave is sent to a DPMZM-based link, the output signal of the DPMZM is written as [11]

$$E_1 = \frac{E_0(\beta_1 e^{j\omega_c t + j\omega_e t} + \beta_1 e^{j\omega_c t - j\omega_e t} + e^{j\omega_c t + j\varphi})}{2} \quad (1)$$

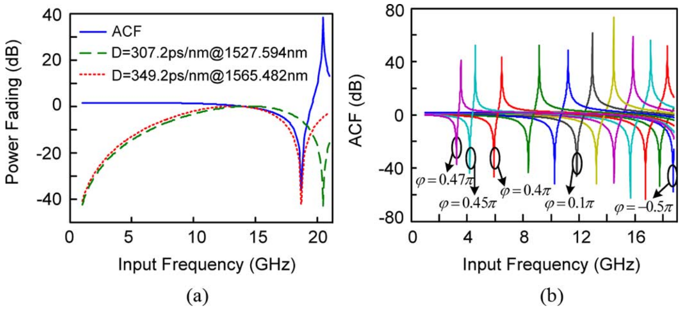

Fig. 2. (a) Power fading functions and the resulted ACF when $\varphi = -0.5\pi$ and (b) The calculated ACF for different φ.

TABLE I
MEASUREMENT RANGE FOR DIFFERENT φ

φ	0.47π	0.45π	0.4π	0.3π	0.2π	0.1π
Measurement range (GHz)	0-3.24	3.24-4.18	4.18-5.92	5.92-8.37	8.37-10.26	10.26-11.84
φ	0.0π	-0.1π	-0.2π	-0.3π	-0.4π	-0.5π
Measurement range (GHz)	11.84-13.24	13.24-14.50	14.50-15.66	15.66-16.75	16.75-17.76	17.76-18.72

where E_0 and ω_c are the amplitude and angular frequency of the lightwave, $\beta_1 = \pi V_e/V\pi_1$ is the modulation index of MZM1, $\varphi = \pi(V_{DC3} - V_0)/V\pi_3$ is the phase bias of MZM3, ω_e and V_e are the angular frequency and amplitude of the RF signal, $V\pi_1$ and $V\pi_3$ are the half-wave voltages of MZM1 and MZM3, V_0 is the offset voltage when $\varphi = 0$. To obtain (1), small-signal modulation is assumed, i.e., $\beta_1 < \pi/6$.

When the signal in (1) is introduced to the SMF, we get

$$E_2 = \frac{E_0 e^{j\omega_c t}(\beta_1 e^{j\omega_e t + j\theta} + \beta_1 e^{-j\omega_e t + j\theta} + e^{j\varphi})}{2} \quad (2)$$

where $\theta = -\pi D\lambda^2 f_e^2/c$, $f_e = \omega_e/2\pi$, and D, λ and c represent the total dispersion of the SMF, the wavelength of the optical carrier and the speed of light in vacuum, respectively.

Applying the optical signal to a PD for square-law detection and ignoring the dc component, we obtain

$$i = \frac{\eta E_0^2 \beta_1 \cos(\omega_e t)\cos(\theta - \varphi)}{2} \quad (3)$$

where η is the responsivity of the PD. Due to the small signal modulation assumption, we also neglect the second-order terms in the PD current.

The power of the obtained RF signal can be thus written as

$$P_o \propto \cos^2\left(\frac{\pi D\lambda^2 f_e^2}{c} + \varphi\right). \quad (4)$$

When two different wavelengths λ_1 and λ_2 are transmitted through the DPMZM-based link, by comparing the microwave powers from the two PDs at the post-processing stage, the amplitude comparison function (ACF) can be obtained

$$ACF = \zeta \frac{\cos^2\left(\frac{\pi D_1 \lambda_1^2 f_e^2}{c} + \varphi\right)}{\cos^2\left(\frac{\pi D_2 \lambda_2^2 f_e^2}{c} + \varphi\right)} \quad (5)$$

where ζ represents the difference of the insertion losses in the two channels, D_1 and D_2 are the total dispersions at the two wavelengths, respectively. By adjusting the optical power of the LDs, we can achieve $\zeta = 1$. From (5), the ACF is monotonically increasing or decreasing from dc to a frequency $f_{\max}$ at which the ACF reaches its extreme value, and has no relationship with the power of the input microwave signal, so f_e can be estimated without ambiguity in this frequency range.

When $-0.5\pi \le \varphi < 0.5\pi$, the highest measurable frequency $f_{\max}$ can be given by

$$f_{\max} = \sqrt{\frac{(0.5\pi - \varphi)c}{(\pi D\lambda^2)_{\max}}} \quad (6)$$

where $(D\lambda^2)_{\max}$ is equal to either $D_1\lambda_1^2$ or $D_2\lambda_2^2$, whichever is larger. Since φ can be easily adjusted by V_{DC3}, the measurement range as well as the resolution can also be tuned by V_{DC3}.

III. SIMULATION AND EXPERIMENTAL RESULTS

Fig. 2(a) shows the simulation results of the power-fading functions and the corresponding ACF when $\varphi = -0.5\pi$. In the simulation, the laser wavelengths are 1527.594 and 1565.482 nm, the length of the SMF is 20 km, and the total dispersions at the two wavelengths are 307.2 and 349.2 ps/nm, respectively. As shown in Fig. 2(a), the variation of the ACF is very small in 0 to $\sim$ 15 GHz. Therefore, the measurement resolution will be very low. Only when the measured microwave frequencies are near the notch point, the measurement resolution will be improved. By simply adjusting V_{DC3} to change φ, the measurement range can be easily tuned. Fig. 2(b) depicts the ACF curves when φ changes from -0.5π to 0.47π with a step of $\sim 0.1\pi$. As can be seen, the notch point of the ACF curve shifts from 3.24 to 18.72 GHz. As a result, by adjusting V_{DC3}, we can select the most suitable ACF curve to measure the frequency in a specific frequency band, which enables us to estimate the microwave frequency with a relatively high resolution over a wide frequency range. The relationship between the measurement range and φ is listed in Table I. With this feature, we can apply the proposed system as the second stage in a two-stage instantaneous frequency measurement scheme. The first stage coarsely determines the frequency band of the intercepted microwave signal, which generates a signal to adjust the phase bias of MZM3, and then the second stage measures the frequency with high resolution. As a result, a wide bandwidth and high resolution instantaneous frequency measurement is achieved.

A proof-of-concept experiment is performed. A tunable laser source (Agilent N7714A), a 22.5 GHz DPMZM (Fujitsu FTM7962EP), a spool of 20-km SMF and a 40 GHz PD are used to construct the DPMZM-based link. The transmission response of the link is measured by a vector network analyzer (VNA, Agilent N5230A). The output power of the electrical signal from the VNA is fixed at 10 dBm. The ACF is achieved by comparing the transmission responses of the link at 1527.594 and 1565.482 nm.

In the experiment, we adjusted V_{DC3} to change φ from -0.5π to 0.47π with a step of $\sim 0.1\pi$. Fig. 3(a) shows the seven typical ACF curves. The calculation and measurement results match very well. Fig. 3(b) shows the measurement frequencies as a function of the input frequency. To obtain the optimized resolution, the frequencies in a specific band are measured by a specific φ. The measured results agree with theoretical values well. Fig. 4 shows the measurement errors

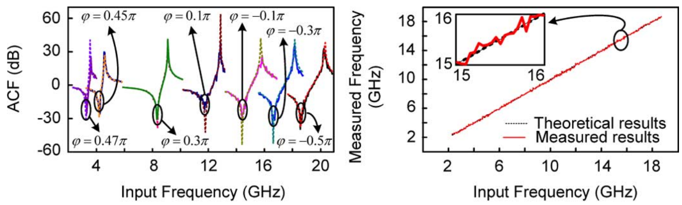

Fig. 3. (a) ACF curves for different φ. Solid lines: the measured curves; dotted lines: the calculated curves. (b) Measured microwave frequencies when the input microwave frequency is tuned from 2.3 to 18.7 GHz. Inset: zoom-in view of the measured microwave frequencies.

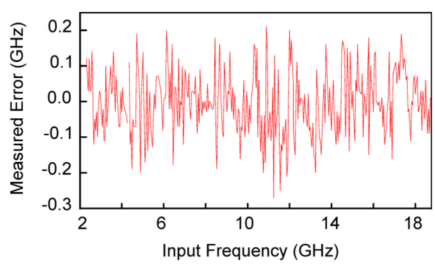

Fig. 4. Distribution of the measurement errors.

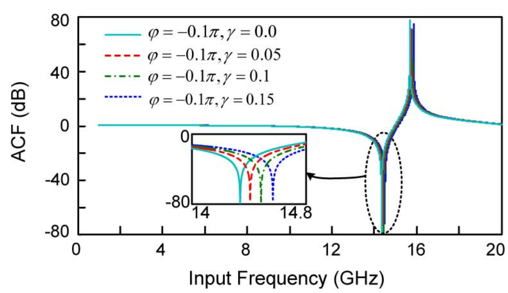

Fig. 5. Calculated ACF curves when $\varphi = -0.1\pi$ and $\gamma = 0$, 0.05, 0.1, or 0.15.

from 2.3 to 18.7 GHz. In the entire measurement range except 11–12 GHz, the measurement error is within ± 0.20 GHz. The dynamic range of the scheme is also studied. The measurement error is within ± 0.20 GHz if the power of the RF signal is in the range from -6 to 14 dBm. The lower bound is limited by the system noise, which can be reduced by applying high-power laser source, while the upper bound is restricted by the nonlinearity of MZM1, which can be linearized by predistortion circuits.

It should be noted that the measurement is almost insensitive to the drift of the bias voltage to MZM2, which changes the optical power in the lower arm of the DPMZM. Assume that MZM2 is not biased at the maximum transmission point, the output signal of the DPMZM is rewritten as

$$E_1 = \frac{E_0(\beta_1 e^{j\omega_c t + j\omega_e t} + \beta_1 e^{j\omega_c t - j\omega_e t} + \alpha e^{j\omega_c t + j\varphi})}{2} \qquad (7)$$

where $0 < \alpha < 1$ is the power attenuation in MZM2. Then, with the similar mathematical manipulation, we can obtain the same ACF expression as (5).

If the bias voltage to MZM1 (i.e., V_{DC1}) is drifted, MZM1 would deviate from the carrier suppressing modulation point. In that case, the output signal of the DPMZM is given by

$$E_1 = \frac{E_0(\beta_1 e^{j\omega_c t + j\omega_e t} + \beta_1 e^{j\omega_c t - j\omega_e t} + \gamma e^{j\omega_c t} + e^{j\omega_c t + j\varphi})}{2} \qquad (8)$$

where $0 < \gamma < 1$, so the ACF is changed to

$$ACF = \zeta \frac{\left[\cos\left(\frac{\pi D_1 \lambda_1{}^2 f_e^2}{c} + \varphi\right) + \gamma \cos\left(\frac{\pi D_1 \lambda_1{}^2 f_e^2}{c}\right)\right]^2}{\left[\cos\left(\frac{\pi D_2 \lambda_2{}^2 f_e^2}{c} + \varphi\right) + \gamma \cos\left(\frac{\pi D_2 \lambda_2{}^2 f_e^2}{c}\right)\right]^2}. \qquad (9)$$

When $\varphi = -0.1\pi$ and $\gamma = 0$, 0.05, 0.1, or 0.15, the calculated ACF curves are shown in Fig. 5. As can be seen, with φ remaining unchanged which means that the nominal measurement range is unchanged, the measurement error increases as the biased voltage V_{DC1} drifts. In the experiment, a 0.8 GHz drift of the ACF curve is observed in an hour. Therefore, a bias stabilization circuit to the MZM1 is required, which is commercially available.

IV. Conclusion

In conclusion, we have proposed and demonstrated a microwave frequency measurement scheme with adjustable measurement range and resolution based on a DPMZM. A measurement range from 2.3 to 18.7 GHz with a measurement error around ± 0.20 GHz was achieved. The proposed scheme features simple structure, low cost and high resolution, which can find application in electronic warfare systems requiring wide bandwidth and high resolution.

References

[1] D. C. Schleher, *Electronic Warfare in the Information Age (Artech House)*. Norwood, MA: , 1999.
[2] L. V. T. Nguyen and D. B. Hunter, "A photonic technique for microwave frequency measurement," *IEEE Photon. Technol. Lett.*, vol. 18, no. 10, pp. 1188–1190, May 2006.
[3] N. Sarkhosh, H. Emami, L. Bui, and A. Mitchell, "Reduced cost photonic instantaneous frequency measurement system," *IEEE Photon. Technol. Lett.*, vol. 20, pp. 1521–1523, Sep. 2008.
[4] M. V. Drummond, P. Monteiro, and R. N. Nogueira, "Photonic RF instantaneous frequency measurement system by means of a polarization-domain interferometer," *Opt. Express*, vol. 17, no. 7, pp. 5433–5438, Mar. 2009.
[5] S. L. Pan and J. P. Yao, "Instantaneous microwave frequency measurement using a photonic microwave filter pair," *IEEE Photon. Technol. Lett.*, vol. 22, no. 19, pp. 1437–1439, Oct. 2010.
[6] X. H. Zou and J. P. Yao, "An optical approach to microwave frequency measurement with adjustable measurement range and resolution," *IEEE Photon. Technol. Lett.*, vol. 20, no. 23, pp. 1989–1991, Dec. 2008.
[7] W. Li, N. H. Zhu, and L. X. Wang, "Reconfigurable instantaneous frequency measurement system based on dual-parallel Mach-Zehnder modulator," *IEEE Photon. J.*, vol. 4, no. 2, pp. 427–436, Apr. 2012.
[8] S. L. Pan and J. P. Yao, "Instantaneous photonic microwave frequency measurement with a maximized measurement range," in *Proc. MWP'09*, Valencia, Spain, 2009, pp. 1–4.
[9] S. Hu, X. Y. Han, P. S. Wu, Y. Y. Gu, and M. S. Zhao, "A photonic technique for microwave frequency measurement employing tunable dispersive medium," in *Proc. MWP'11*, Singapore, 2011, pp. 165–168.
[10] H. L. Zhang and S. L. Pan, "Instantaneous frequency measurement with adjustable measurement range and resolution based on polarisation modulator," *Electron. Lett.*, vol. 49, no. 4, pp. 277–279, Feb. 2013.
[11] S. Y. Li, X. P. Zheng, H. Y. Zhang, and B. K. Zhou, "Compensation of dispersion-induced power fading for highly linear radio-over-fiber link using carrier phase-shifted double sideband modulation," *Opt. Lett.*, vol. 36, no. 4, pp. 546–548, Feb. 2011.